http://ansinet.com/itj

ITJ

ISSN 1812-5638

INFORMATION TECHNOLOGY JOURNAL

ANSInet
Asian Network for Scientific Information
308 Lasani Town, Sargodha Road, Faisalabad - Pakistan

Information Technology Journal 8 (3): 347-353, 2009
ISSN 1812-5638

Steady-State Modeling of Static Synchronous Compensator and Thyristor Controlled Series Compensator for Power Flow Analysis

[1]M.O. Hassan, [1]S.J. Cheng and [2]Z.A. Zakaria
[1]Department of Electrical Engineering, Huazhong University of Science and Technology, Wuhan, China
[2]School of Electrical Engineering, Wuhan University, Wuhan, China

Abstract: In this study, steady-state modeling of Static Synchronous Compensator (STATCOM) and Thyristor Controlled Series Compensator (TCSC) for power flow studies has been represented. STATCOM is modeled as a controllable voltage source in series with impedance and firing angle model for TCSC is used to control active power flow of the line to which TCSC is installed. Proposed model for TCSC takes firing angle as state variable in power flow formulation. To validate the effectiveness of the proposed models Newton-Raphson method algorithm was implemented to solve power flow equations in presence of STATCOM and TCSC. Case studies are carried out on 9-bus system to demonstrate the performance of the proposed models. Simulation results show the effectiveness and robustness of the proposed models; moreover the power solution using the Newton-Raphson algorithm developed incorporating firing angle model possesses excellent convergence characteristics.

Key words: Static synchronous compensator, thyristor controlled series compensator, power flow, steady-state modeling, Newton-Raphson

INTRODUCTION

With the rapid development of power system, especially the increased use of transmission facilities due to higher industrial output and deregulation, it becomes necessary to explore new ways of maximizing power transfer in existing transmission facilities, while at the same time maintaining the acceptable levels of the network reliability and stability. On the other hand, the fast development of power electronic technology has made FACTS (flexible AC Transmission system) promising solution of future power system. FACTS controllers such as Static Synchronous Compensator (STATCOM), Static VAR Compensator (SVC), Thyristor Control Series Compensator (TCSC), Static Synchronous Series Compensator (SSSC) and Unified Power Flow Controller (UPFC) are able to change the network parameters in a fast and effective way in order to achieve better system performance (Hingorani and Gyugyi, 1999; Edris, 2000; Mohan Marthur and Rajiv Varma, 2002). These controllers are used for enhancing dynamic performance of power systems in terms of voltage/angle stability while improving the power transfer capability and voltage profile in steady state (Kirschner *et al*., 2005; Yan and Singh, 2001; Perez *et al*., 2000; Xingbin *et al*., 2003).

Static Synchronous Compensators (STATCOM) and Thyristor-Controlled Series Capacitor (TCSC) are members of FACTS family that have successfully been used in power systems to improve both the steady state and dynamic performance of the systems.

Static Synchronous Compensator (STATCOM) compensate the reactive power from or to the power system. This function is identical to the synchronous condenser with rotating mass, but its response time is extremely faster than of the synchronous condenser. This rapidity is very effective to increase transient stability, enhance voltage support and to damp low frequency oscillation for transmission system.

Thyristor-Controlled Series Capacitor (TCSC) is an important component of FACTS. With the firing control of the thyristors, it can change its apparent reactance smoothly and rapidly. The TCSC is able to directly schedule the real power flow through a typically selected line and allow the system to operate closer to the line limits. More importantly because of its rapid and flexible regulation ability, it can improve transient stability and dynamic performance of the power systems. Particularly, in systems with large bulk transfer of power and long transmission lines it can be used to increase the power transfer capability and damp low frequency oscillations.

Now, for maximum utilization of any FACTS device in power system planning, operation and control, power flow solution of the network that contains any of these devices is a fundamental requirement, As a result, many

Corresponding Author: Mohammed Osman Hassan, Department of Electrical Engineering, Huazhong University of Science and Technology, Wuhan, China

excellent research studies have been carried out in the literature for developing efficient load flow algorithm for FACTS devices (Narayana and Abdel Moamen, 2005; Yan and Sekar, 2005).

This study focuses on the development of STATCOM and TCSC models and their implementation in Newton-Raphson load flow algorithm, to control voltage of the bus and active power across the line.

POWER FLOW EQUATION

Basically load flow problem involves solving the set of non-linear algebraic equations which represent the network under steady state conditions. The reliable solution of real life transmission and distribution networks is not a trivial matter and Newton-type methods, with their strong convergence characteristics, have proved most successful. To illustrate the power flow equations, the power flow across the general two-port network element connecting buses k and m shown in Fig. 1 is considered and the following equations are obtained.

The injected active and reactive power at bus-k (P_k and Q_k) is:

$$P_k = G_{kk} V_k^2 + (G_{km} \cos\delta_{km} + B_{km} \sin\delta_{km}) V_k V_m \quad (1)$$

$$Q_k = -B_{kk} V_k^2 + (G_{km} \sin\delta_{km} - B_{km} \cos\delta_{km}) V_k V_m \quad (2)$$

$$P_k = G_{mm} V_m^2 + (G_{mk} \cos\delta_{mk} + B_{mk} \sin\delta_{mk}) V_k V_m \quad (3)$$

$$Q_k = -B_{mm} V_k^2 + (G_{mk} \sin\delta_{mk} - B_{mk} \cos\delta_{mk}) V_k V_m \quad (4)$$

Where:

$\delta_{km} = \delta_k - \delta_m = -\delta_m$

$Y_{kk} = Y_{mm} = G_{kk} + jB_{kk} = Y_{ko} + Y_{km}$

$Y_{km} = Y_{mk} = G_{km} + jB_{km} = -Y_{mk}$

The nodal power flow equations:

$$P = f(V, \theta, G, B)$$
$$Q = g(V, \theta, G, B) \quad (5)$$

and their linearisation around a base point, (P^0,Q^0):

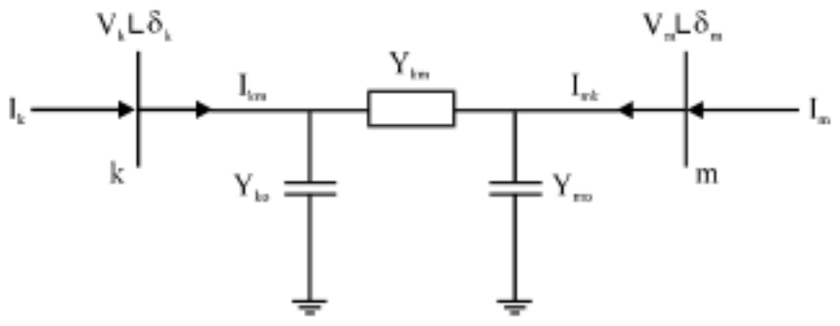

Fig. 1: General two-port network

$$\begin{bmatrix} \Delta P \\ \Delta Q \end{bmatrix}^i = [J]^i \begin{bmatrix} \Delta\theta \\ \Delta V \end{bmatrix}^i \quad (6)$$

where, P and Q are vectors of real and reactive nodal power injections as a function of nodal voltage magnitudes V and angles θ and network conductances G and suceptances B.

$\Delta P = P_{spec} - P_{cal}$ is the real power mismatch vector, $\Delta Q = Q_{spec} - Q_{cal}$ is the reactive power mismatch vector, $\Delta\theta$ and ΔV are the vectors of incremental changes in nodal voltage magnitudes and angles, J is the matrix of partial derivatives of real and reactive powers with respect to voltage magnitudes and angles and i indicates the iteration number.

Incorporation of FACTS devices in an existing load flow algorithm results in increased complexity of programming due to the following reasons (Suman *et al*., 2007):

- New terms owing to the contributions from the FACTS devices need to be included in the existing power flow equations of the concerned buses. These terms necessitate modification of existing power flow codes
- New power flow equations related to the FACTS devices come into the picture, which dictate formulation of separate subroutine(s) for computing them
- The system Jacobian matrix contains entirely new Jacobian sub-blocks exclusively related to the FACTS devices. Therefore, new codes have to be written for computation of these Jacobian sub-blocks

The increase in the dimension of Jacobian matrix, compared with the case when there are no power system controllers, is proportional to the number and kind of such controllers. The simultaneous equations for the network and power system state variables are (Acha *et al*., 2004):

$$\left.\begin{aligned} f(X_{nsys}, R_{nF}) = 0 \\ g(X_{nsys}, R_{nF}) = 0 \end{aligned}\right\} \quad (7)$$

Where:

X_{nsys} = Network state variables i.e., (voltage magnitudes and phase angles)

R_{nF} = Power system controller variables

The structure of the modified Jacobian incorporated FACTS controller is shown in Fig. 2.

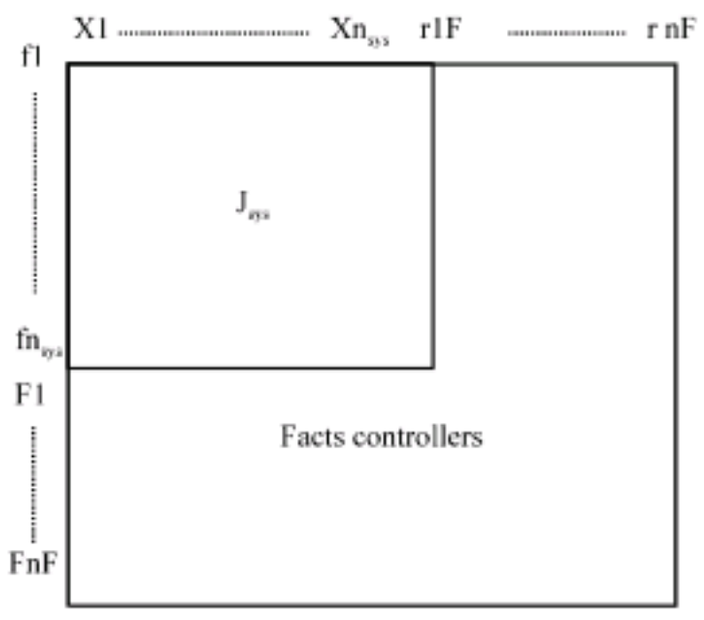

Fig. 2: Modified Jacobian incorporated FACTS controllers

POWER SYSTEM WITH STATCOM

Figure 3 shows the circuit model of a STATCOM connected to Bus k of an N-Bus power. The STATCOM is modeled as a controllable voltage source (E_{stat}) in series with impedance (Ying *et al*., 2002). The real part of this impedance represents the ohmic losses of the power electronic devices and the coupling transformer, while the imaginary part of this impedance represents the leakage reactance of the coupling transformer. Assume that the STATCOM is operating in voltage control mode. This means that the STATCOM absorbs proper amount of reactive power from the power system to keep $|V_k|$ constant for all power system loading within reasonable range. The ohmic loss of the STATCOM is accounted by considering the real part of Y_{stat} in power flow calculations. The net active/reactive power injection at Bus k including the local load, before addition of the STATCM, is shown by P_k+jQ_k.

The power flow equations of the system with STATCOM connected to Bus k, can written as:

$$P_K = P_{stat} + \sum_{j=1}^{N} |V_k||V_j||Y_{kj}|\cos(\delta_k - \delta_j - \theta_{kj}) \quad (8)$$

$$Q_K = Q_{stat} + \sum_{j=1}^{N} |V_k||V_j||Y_{kj}|\sin(\delta_k - \delta_j - \theta_{kj}) \quad (9)$$

$$P_{stat} = G_{stat}|V_k|^2 - |V_k||E_{stat}||Y_{stat}|\cos(\delta_k - \delta_{stat} - \theta_{stat}) \quad (10)$$

$$Q_{stat} = B_{stat}|V_k|^2 - |V_k||E_{stat}||Y_{stat}|\sin(\delta_k - \delta_{stat} - \theta_{stat}) \quad (11)$$

where, $|E_{stat}|$, δ_{stat}, $|Y_{stat}|$ and θ_{stat} are shown in Fig. 3.

Addition of STATCOM introduces two new variables $|E_{stat}|$ and δ_{stat}; however, $|V_k|$ is now known. Thus, one more equation is needed to solve the power flow problem. Equation 11 is found using the fact that the power

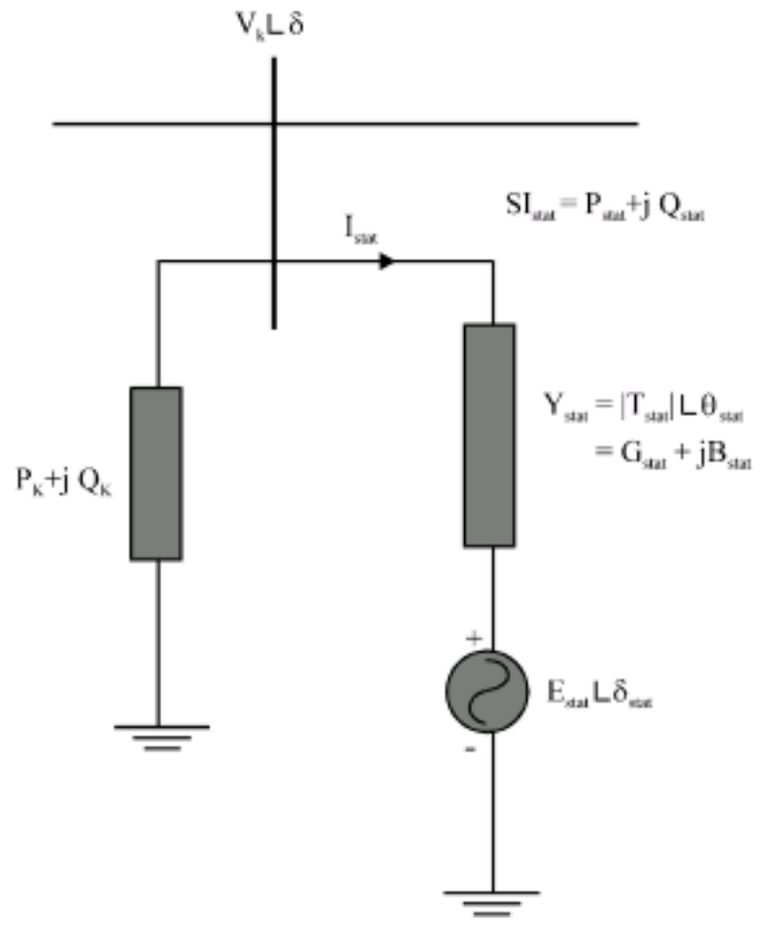

Fig. 3: Steady state model of STATCOM

consumed by the source E_{stat} (P_{Estat}) must be zero in steady state. Thus the equatioin for P_{Estat} is can written as:

$$P_{E_{stat}} = \text{Real}\left[E_{stat}I_{stat}^{*}\right] = -G_{stat}|E_{stat}|^2 + |E_{stat}||V_k||Y_{stat}|\cos(\delta_{stat} - \delta_k - \theta_{stat}) = 0 \quad (12)$$

Using these power equations, the linearized STATCOM model is given below:

$$\begin{bmatrix} \Delta P_k \\ \Delta Q_k \\ \Delta P_{stat} \\ \Delta Q_{stat} \end{bmatrix} = \begin{bmatrix} \frac{\partial P_k}{\partial \theta_k} & \frac{\partial P_k}{\partial V_k}V_k & \frac{\partial P_k}{\partial \delta_{stat}} & \frac{\partial P_k}{\partial V_{stat}}V_{stat} \\ \frac{\partial Q_k}{\partial \theta_k} & \frac{\partial Q_k}{\partial V_k}V_k & \frac{\partial Q_k}{\partial \delta_{stat}} & \frac{\partial Q_m}{\partial V_{stat}}V_{stat} \\ \frac{\partial P_{stat}}{\partial \theta_k} & \frac{\partial P_{stat}}{\partial V_k}V_k & \frac{\partial P_{stat}}{\partial \delta_{stat}} & \frac{\partial P_{stat}}{\partial V_{stat}}V_{stat} \\ \frac{\partial Q_{stat}}{\partial \theta_k} & \frac{\partial Q_{stat}}{\partial V_k}V_k & \frac{\partial Q_{stat}}{\partial \delta_{stat}} & \frac{\partial Q_{stat}}{\partial V_{stat}}V_{stat} \end{bmatrix} \begin{bmatrix} \Delta\theta_k \\ \frac{\Delta V_k}{V_k} \\ \Delta\delta_{stat} \\ \frac{\Delta V_{stat}}{V_{stat}} \end{bmatrix} \quad (13)$$

where, the voltage magnitude and phase angle are taken to be state variables.

MODELING OF THYRISTOR CONTROLLED SERIES COMPENSATOR

Thyristor-Controlled Series Compenator (TCSC) allows rapid and continuous changes of transmission line impedance. Figure 4 shows the TCSC module connected in series with the transmission line. The structure of the controller is equivalent to the FC-TCR SVC. However, the equivalent impedance of the TCSC at 60 Hz is more appropriately represented by assuming a sinusoidal steady-state total current rather than a sinusoidal voltage.

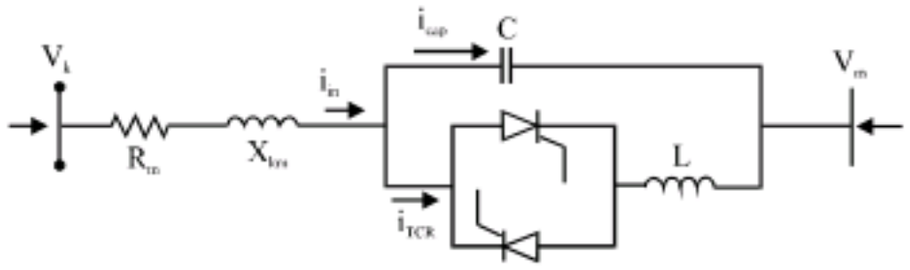

Fig. 4: TCSC module

In this study, TCSC is represented by its fundamental frequency impedance. The TCSC linearized power flow equations, with respect to the firing angle, are incorporated into an existing Newton-Raphson algorithm. Since the explicit information about the TCSC impedance-firing angle is available, good initial conditions are easily selected, hence preventing load flow iterative process from entering the nonoperative regions owing to the presence of resonant bands. The fundamental TCSC equivalent reactance is given as:

$$X_{TCSC} = -X_C + K_1(2\sigma + \sin 2\sigma - K_2\cos^2\sigma(\varpi\tan\varpi\sigma) - \tan\sigma) \quad (14)$$

Where:
$\sigma = \pi - \alpha$

$$\begin{aligned} X_{LC} &= \frac{X_C X_L}{X_C - X_L} \\ K_1 &= \frac{X_C + X_{LC}}{\pi} \\ K_2 &= \frac{(X_{LC})^2}{\pi X_L} \end{aligned} \quad (15)$$

The behavior of TCSC power flow model is influenced greatly by the number of resonant points which can be given as:

$$\alpha = \pi\left(1 - \frac{(2n-1)\omega\sqrt{LC}}{2}\right) \quad (16)$$

where, n = 1, 2, 3....

It should be noted that near resonant point, a small variations in the firing angle will induce large changes in both X_{tcsc} and $\partial X_{tcsc}/\partial\alpha$. This in turn may lead to ill conditioned TCSC power equations.

To develop TCSC model, suppose the transmission line admittance in which TCSC is connected is:

$$G_{tcsc} + jB_{tcsc} = \frac{1}{R + j(X + X_{tcsc})} \quad (17)$$

Power flow equations of the line k-m in which TCSC is placed is given by:

$$P_{km}^{tcsc} = V_k^2 G_{tcsc} - V_k V_m\left(G_{tcsc}\cos(\delta_{km}) + B_{tcsc}\sin(\delta_{km})\right) \quad (18)$$

When TCSC is used to control power flow in the line k-m, the set of linearised power flow equations are given by:

$$\begin{bmatrix} \Delta P_k \\ \Delta P_m \\ \Delta Q_k \\ \Delta Q_m \\ \Delta P_{km}^{tcsc} \end{bmatrix} = \begin{bmatrix} \frac{\partial P_k}{\partial\theta_k} & \frac{\partial P_k}{\partial\theta_m} & \frac{\partial P_k}{\partial V_k}V_k & \frac{\partial P_k}{\partial V_m}V_m & \frac{\partial P_k}{\partial\alpha} \\ \frac{\partial P_m}{\partial\theta_k} & \frac{\partial P_m}{\partial\theta_m} & \frac{\partial P_m}{\partial V_k}V_k & \frac{\partial P_m}{\partial V_m}V_m & \frac{\partial P_m}{\partial\alpha} \\ \frac{\partial Q_k}{\partial\theta_k} & \frac{\partial Q_k}{\partial\theta_m} & \frac{\partial Q_k}{\partial V_k}V_k & \frac{\partial Q_k}{\partial V_m}V_m & \frac{\partial Q_k}{\partial\alpha} \\ \frac{\partial Q_m}{\partial\theta_k} & \frac{\partial Q_m}{\partial\theta_m} & \frac{\partial Q_m}{\partial V_k}V_k & \frac{\partial Q_m}{\partial V_m}V_m & \frac{\partial Q_m}{\partial\alpha} \\ \frac{\partial P_{km}^{tcsc}}{\partial\theta_k} & \frac{\partial P_{km}^{tcsc}}{\partial\theta_m} & \frac{\partial P_{km}^{tcsc}}{\partial V_k}V_k & \frac{\partial P_{km}^{tcsc}}{\partial V_m}V_m & \frac{\partial P_{km}^{tcsc}}{\partial\alpha} \end{bmatrix} \begin{bmatrix} \Delta\theta_k \\ \Delta\theta_m \\ \frac{\Delta V_k}{V_k} \\ \frac{\Delta V_m}{V_m} \\ \Delta\alpha \end{bmatrix} \quad (19)$$

where, the elements of additional row and column of the modified Jacobean can be written as:

$$\frac{\partial P_k}{\partial\alpha} = V_k V_m\left(-\frac{\partial G_{tcsc}}{\partial\alpha}\cos(\delta_{km}) - \frac{\partial B_{tcsc}}{\partial\alpha}\sin(\delta_{km})\right) - V_k^2\frac{\partial X_{tcsc}}{\partial\alpha} \quad (20)$$

$$\frac{\partial Q_k}{\partial\alpha} = V_k V_m\left(-\frac{\partial G_{tcsc}}{\partial\alpha}\sin(\delta_{km}) - \frac{\partial B_{tcsc}}{\partial\alpha}\cos(\delta_{km})\right) - V_k^2\frac{\partial X_{tcsc}}{\partial\alpha} \quad (21)$$

Where:

$$\frac{\partial G_{tcsc}}{\partial\alpha} = \frac{-2R(X + X_{tcsc})}{\left(R^2 + (X + X_{tcsc})^2\right)^2}\frac{\partial X_{tcsc}}{\partial\alpha} \quad (22)$$

$$\frac{\partial B_{tcsc}}{\partial\alpha} = -\frac{1}{\left(R^2 + (X + X^{tcsc})^2\right)^2}\left(\frac{\partial X_{tcsc}}{\partial\alpha}\right) + \frac{2(X + X_{tcsc})^2}{\left(R^2 + (X + X_{tcsc})^2\right)^2}\left(\frac{\partial X_{tcsc}}{\partial\alpha}\right) \quad (23)$$

$$\begin{aligned} \frac{\partial X_{tcsc}}{\partial\alpha} &= -2C_1(1 + \cos 2\alpha) + C_2\sin(2\alpha)\left(\varpi\tan(\varpi(\pi - \alpha)) + \tan\alpha\right) \\ &+ C_2\left(\varpi^2\frac{\cos^2(\pi - \alpha)}{\cos^2(\varpi(\pi - \alpha))} - 1\right) \end{aligned} \quad (24)$$

Also the elements of the added row in Eq. 19 can be written as:

$$\frac{P_{km}^{tcsc}}{\partial\alpha} = V_k^2\frac{G_{tcsc}}{\partial\alpha} - V_k V_m\left(\frac{G_{tcsc}}{\partial\alpha}\cos(\delta_{km}) + \frac{B_{tcsc}}{\partial\alpha}\sin(\delta_{km})\right) \quad (25)$$

$$\frac{P_{km}}{\partial\delta_k} = -V_k V_m\left(-G_{tcsc}\sin(\delta_{km}) + B_{tcsc}\cos(\delta_{km})\right) \quad (26)$$

$$\frac{\partial P_{km}^{tcsc}}{\partial\delta_m} = \frac{\partial P_{km}^{tcsc}}{\partial\delta_k} \quad (27)$$

$$\frac{\partial P_{km}^{tcsc}}{\partial V_k}V_k = P_{km}^{tcsc} + V_k^2 G_{tcsc} \quad (28)$$

$$\frac{\partial P_{km}^{tcsc}}{\partial V_m} V_m = P_{km}^{tcsc} - V_k^2 G_{tcsc} \quad (29)$$

In the mismatch vector of (18):

$\Delta P_{km}^{tcsc} = P_{km}^{req} - P_{km}^{tcsc}$ is the active power flow mismatch for the TCSC module and P_{km}^{req} is the required power flow in the TCSC branch.

Now solve for system variables along with the firing angle mismatch using Eq. 19, making use of modified Jacobean matrix. Update the firing angles using the following equation

$$\alpha^{i+1} = \alpha^{i} + \Delta\alpha$$

where, $\Delta\alpha$ is the incremental change in the TCSC's firing angle and i shows ith iteration.

SIMULATION AND RESULTS

A 9-bus system is used to assess the effectiveness of Statcom and TCSC models developed in this study. Figure 5 shows the single line diagram of system, with 230 kV and 100MVA base has been considered. The data of the generator, load, transformer and line data are given in (Anderson and Fouad, 2002). Five cases are considered, statcom is connected at bus 8 and then at bus 5 and finally at bus 6, TCSC connected between line 7-8 and then between line 9-8.

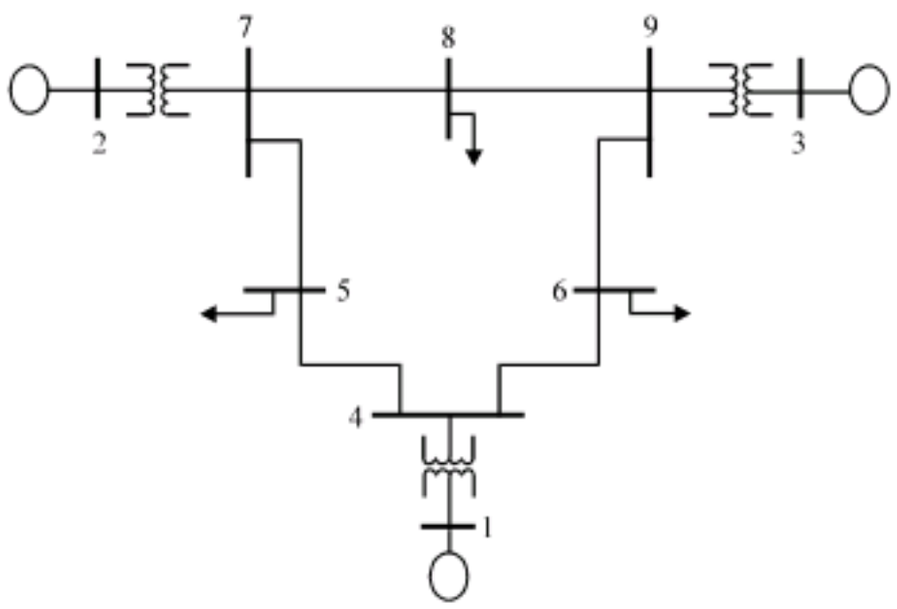

Fig. 5: 9-bus system

Case 1: Statcom is connected to bus 8, the control aim to keep the voltage at that bus at 1.0 pu. The value X_{stat} is chosen as 0.14 pu. The convergent is obtained after 6 iterations. statcom absorbs 21.86 MAVR from bus 8 in order to keep the voltage magnitude at 1 pu, the associated values of E_{stat} and δ_{stat} are 0.9694 pu and 0.8268°, respectively. Table 1 shows the voltage magnitude and phase angle for all buses of the system with and without STATCOM

Case 2: Statcom is connected to bus 5, the control aim to keep the voltage at that bus at 1.0 pu. The value X_{stat} is chosen as 0.3 pu. The convergent is obtained after 6 iterations. statcom injects 4.84 MAVR in bus 8 in order to keep the voltage magnitude at 1 pu, the associated values of E_{stat} and δ_{stat} are 1.0145 pu and -3.989°, respectively (Table 1).

Case 3: Statcom is connected to bus 6, to keep the voltage at bus 6 at 1.0 pu. The value X_{stat} is chosen as 0.2 pu. The convergent is obtained after 6 iterations. statcom absorbs 13.72 MAVR from bus 6 in order to keep the voltage magnitude at 1 pu, the associated values of E_{stat} and δ_{stat} are 0.9726 pu and -3.646°, respectively. The voltage magnitude and phase angle for all buses of the system are shown in Table 1.

Case 4: TCSC is connected between bus 7 and 8, the control aim is to increase the real power flows in line 7-8 to 80 MW. The of values X_C and X_L are chosen as 9.522 Ω pu and 1.9 Ω with these values there is only one resonant point at $\alpha = 139.75°$, firing angle is set initially at 146°, which lies on the capacitive region of TCSC. After running load flow program X_{tcsc} is equal to -0.0319 and the final firing angle value is 149.029^0. Table 2 power flow results of 9-bus system

Table 1: Voltage magnitude and phase angle for 9-bus system with and without STATCOM

	Bus								
Magnitude and angle	1	2	3	4	5	6	7	8	9
No facts									
V	1.0400	1.0250	1.0250	1.0258	0.9956	1.0127	1.0258	1.0159	1.0324
δ	0.0000	9.2800	4.6648	-2.2168	-3.9888	-3.6874	3.7197	0.7275	1.9667
STATCOM at bus 8									
V	1.0400	1.0250	1.0250	1.0236	0.9916	1.0092	1.0189	1.0000	1.0269
δ	0.0000	9.4248	4.7394	-2.2257	-3.9983	-3.6956	3.8269	0.8268	2.0270
STATCOM at bus 5									
V	1.0400	1.0250	1.0250	1.0274	1.0000	1.0140	1.0269	1.0167	1.0328
δ	0.0000	9.2720	4.6722	-2.2121	-3.9886	-3.6762	3.7176	0.7339	1.9754
STATCOM at bus 6									
V	1.0400	1.0250	1.0250	1.0213	0.9920	1.0000	1.0243	1.0138	1.0295
δ	0.0000	9.2759	4.6707	-2.2290	-4.0201	-3.6458	3.7077	0.7114	1.9650

Table 2: Power flow results of 9-bus system with and without TCSC

	Line	
Power flow results	7-8	9-8
Final firing angle value (°)	149.0300	149.2400
X_{tcsc} (pu)	-0.0319	-0.0439
Compensation (%)	-44.3000	-43.6000
Active power without TCSC (MW)	76.3800	24.1800
Active power with TCSC (MW)	80.0000	26.0000

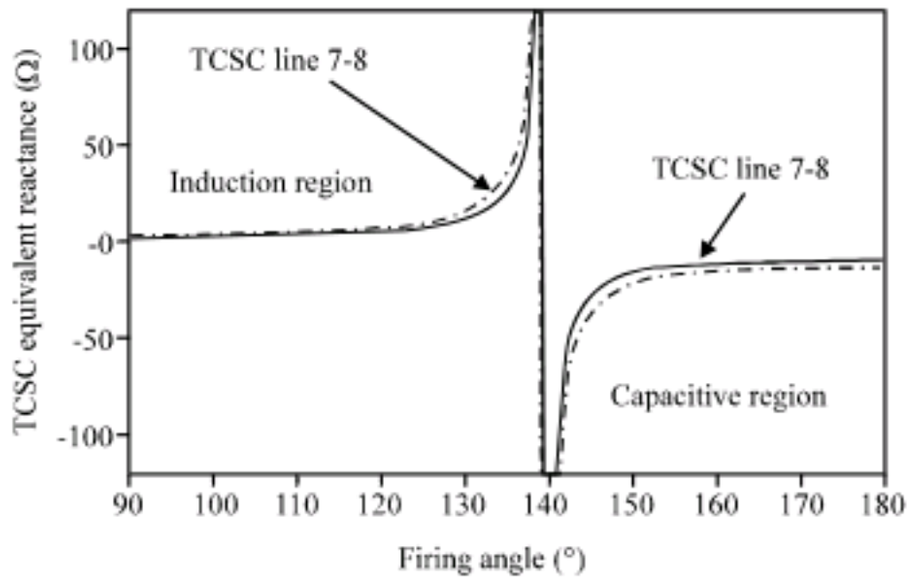

Fig. 6: Reactance-firing angle characteristics

with and without TCSC and Fig. 6 shows reactance-firing angle characteristics. From Table 2, real power flow in line 7-8 at sending end increased from 76.38 to 80 MW.

Case 5: TCSC is connected between bus 9 and 8, the control aim is to increase the real power flows in line 9-8 to 26 MW. The of values X_C and X_L are chosen as 13.33 Ω pu and 2.67 Ω with these values there is only one resonant point at $\alpha = 139.75°$, firing angle is set initially at 146^0, which lies on the capacitive region of TCSC. After running load flow program X_{tcsc} is equal to -0.0439 and the final firing angle value is 149.24°. The power flow results are tabulated as shown in Table 2, Figure 6 shows reactance-firing angle characteristics. From Table 2, real power flow in line 9-8 at sending end increased from 76.38 to 80 MW.

CONCLUSION

In this study, steady-state models of STATCOM and TCSC for power flow solution were developed and discussed in details. STATCOM is modeled as a controllable voltage source in series with impedance where the voltage magnitude E_{stat} and phase angle δ_{stat} are taken to be state variables in power flow formulation, while firing angle model for TCSC is used to control active power flow of the line to which TCSC is installed. To demonstrate the effectiveness and robustness of the proposed models, a Newton-Raphson method incorporating firing angle model for STATCOM and TCSC was developed for desired power transferred and bus voltage profile improvement. Then the proposed models and algorithm were implemented on IEEE 9-bus system for different case studies. The results obtained show the effectiveness and robustness of the proposed models; moreover the power solution using the Newton-Raphson algorithm developed incorporating firing angle model possesses excellent convergence characteristics.

REFERENCES

Acha, E., R. Claudio, E. Fuerte, H. Ambriz-Pérez and C. Angeles-Camacho, 2004. FACTS: Modeling and Simulation in Power Networks. 1st Edn., John Wiley and Sons, Inc., USA., ISBN: 978-0-470-85271-2.

Anderson, P.M. and A.A. Fouad, 2002. Power System Control and Stability. 2nd Edn., Wiley-IEEE Press, New York, ISBN-13: 978-0471238621, pp: 672.

Edris, 2000. FACTS technology development: An update. IEEE Eng. Rev., 20: 4-9.

Hingorani, N.G. and L. Gyugyi, 1999. Understanding FACTS: Concepts and Technology of Flexible AC Transmission Systems. 1st Edn., IEEE Press, New York, ISBN-10: 0780334558.

Kirschner, L., D. Retzmann and G. Thumm, 2005. Benefits of FACTS for power system enhancement. Proceedings of the IEEE PES Transmission and Distribution Conference and Exhibition: Asia and Pacific, 2005 IEEE, Dalian, pp: 1-7.

Mohan Marthur, R. and K. Rajiv Varma, 2002. Thyristor Based-FACTS Controllers for Electrical Transmission Systems. 1st Edn., Wiley, USA., ISBN-10: 0471206431.

Narayana, P.P. and M.A. Abdel Moamen, 2005. Power flow control and solutions with multiple and multi-type FACTS devices. Elect. Power Sys. Res., 74: 341-351.

Perez, M.A., A.R. Messina and C.R. Fuerte-Esquivel, 2000. Application of FACTS devices to improve steady state voltage stability. Proceedings of the Power Engineering Society Summer Meeting, Jul. 16-20, IEEE, Seattle, WA, USA., pp: 1115-1120.

Suman, B., B. Das and N. Kumar, 2007. An indirect model of SSSC for reducing complexity of coding in Newton power flow algorithm. Elect. Power Sys. Res., 77: 1432-1441.

Xingbin, Y., C. Singh, S. Jakovljevic, D. Ristanovic and G. Huang, 2003. Total transfer capability considering FACTS and security constraints. Proceedings of the IEEE PES Transmission and Distribution Conference and Exposition, Sept. 7-12, IEEE pp: 73-78.

Yan, O. and C. Singh, 2001. Improvement of total transfer capability using TCSC and SVC. Proceedings of the Power Engineering Society Summer Meeting, Jul. 15-19, IEEE Publication, Vancouver, BC, Canada,-pp: 944.

Yan, P. and A. Sekar, 2005. Steady state analysis of power system having multiple FACTS devices using line-flow based equations. IEEE Pro. Transm. Distrib., 152: 31-39.

Ying, X., Y.H. Song and Y.Z. Sun, 2002. Power flow control approach to power systems with embedded FCATS devices. IEEE Trans. Power Syst., 17: 934-950.